a

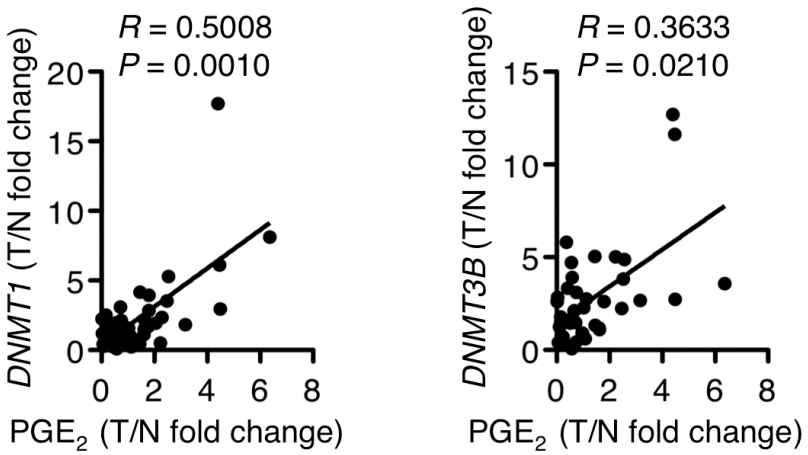

b

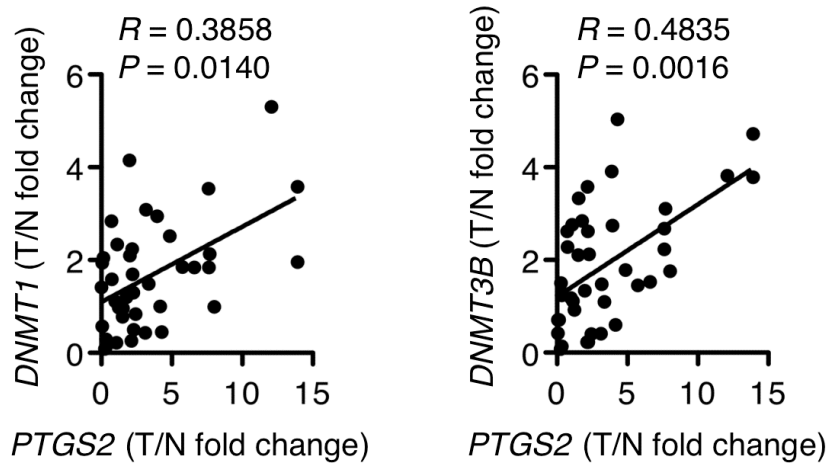

Supplementary Figure 1 The correlation between levels of PTGS2, PGE_2, DNMT1, and DNMT3B in human CRC. (**a**,**b**) The levels of PGE_2 (**a**) and *PTGS2* (*COX-2*) mRNA (**b**) are correlated with the expression of *DNMT1* and *DNMT3B* at mRNA levels in 40 pairs of human colorectal carcinomas (T) with matched normal tissues (N). Data were presented as fold changes in cancer specimens as compared to matched normal tissues. Nonparametric Spearman correlation analysis (*R* value) was performed.

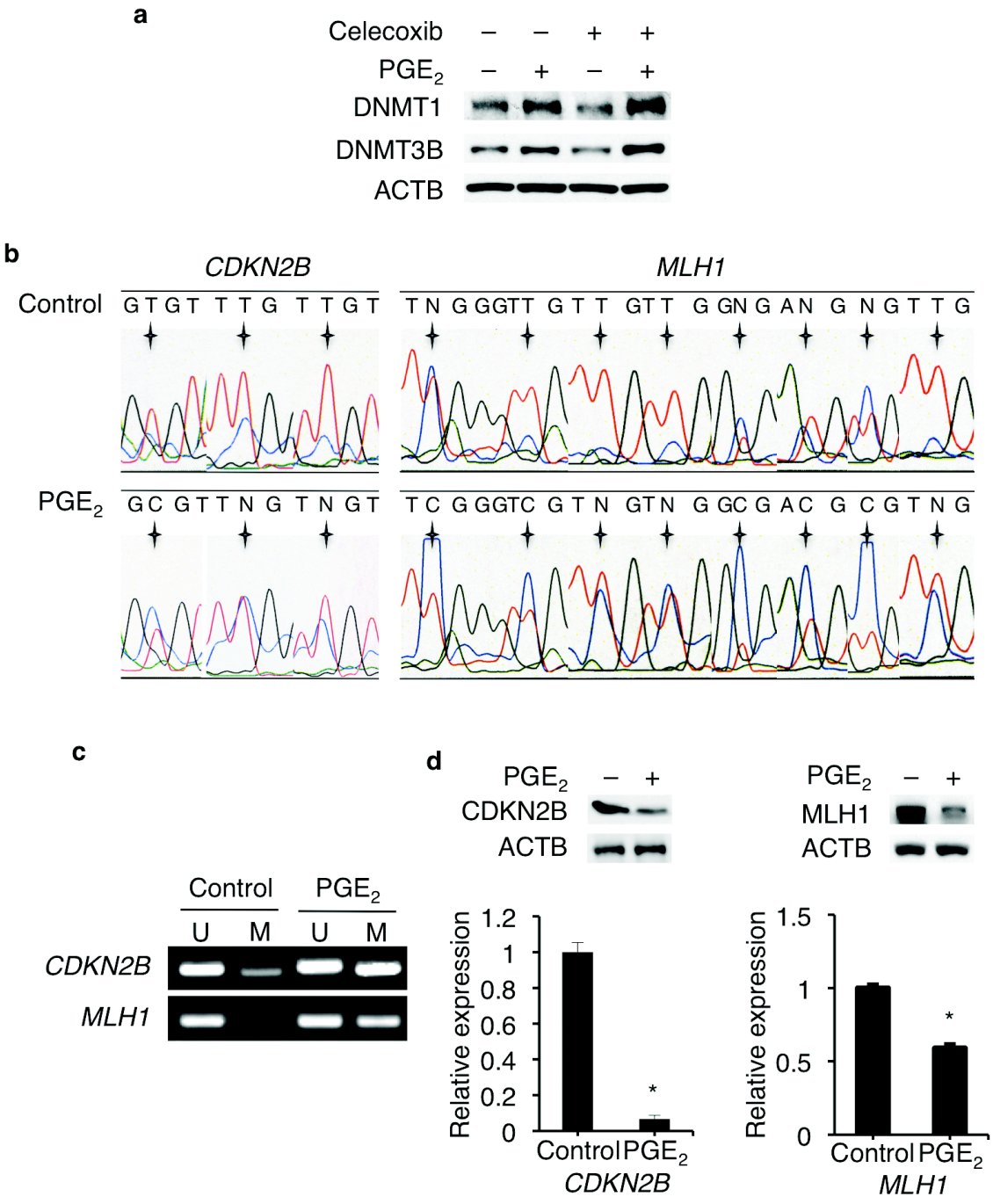
a
Celecoxib – – + +
PGE2 – + – +
DNMT1
DNMT3B
ACTB
b
CDKN2B
MLH1
Control
PGE2
c
Control PGE2
U M U M
CDKN2B
MLH1
d
PGE2 – +
CDKN2B
ACTB
MLH1
Relative expression
Control PGE2
CDKN2B
MLH1
e
shDNMT1
shDNMT3B
shCon C1 C2 shCon C1 C2
PGE2 – + – + – + – + – + – +
CDKN2B
MLH1
ACTB

Supplementary Figure 2 PGE_2 silences *CDKN2B* (*p15*) and *MLH1* genes by enhancing the promoter CGI methylation of these genes in human CRC cell lines. (**a**) PGE_2 attenuated the effect of celecoxib on downregulating DNMT1 and DNMT3B protein expression in HT-29 cells. (**b**) PGE_2 increased the promoter CGI methylation of *CDKN2B* (*p15*) and *MLH1* in LS-174T cells. For *CDKN2B* (*p15*) promoter, a region (–3 to +247) that contains 27 CpGs was examined. Three representative CpGs were presented. For the *MLH1* promoter, a region (–401 to –113) that contains 19 CpGs was examined. Eight representative CpGs were presented. (**c**) PGE_2-enhanced CGI methylation of *CDKN2B* (*p15*) and *MLH1* in LS-174T cells was measured by methylation-specific PCR (MSP). U: unmethylated PCR products with primers targeting unmethylated template sequences. M: methylated PCR products with primers targeting methylated template sequences. (**d**) PGE_2 decreased the expression of CNR1 (CB1) and MGMT at both protein and mRNA levels. The levels of protein (upper panels) and mRNA (lower panels) were examined as described in **Fig. 1c**. (**e**) Knockdown of *DNMT1* or *DNMT3B* attenuated PGE_2-indiuced downregulation of CDKN2B (p15) and MLH1 in LS-174T cells. CDKN2B (p15) and MLH1 protein expression was examined as described in **Fig. 1e**.

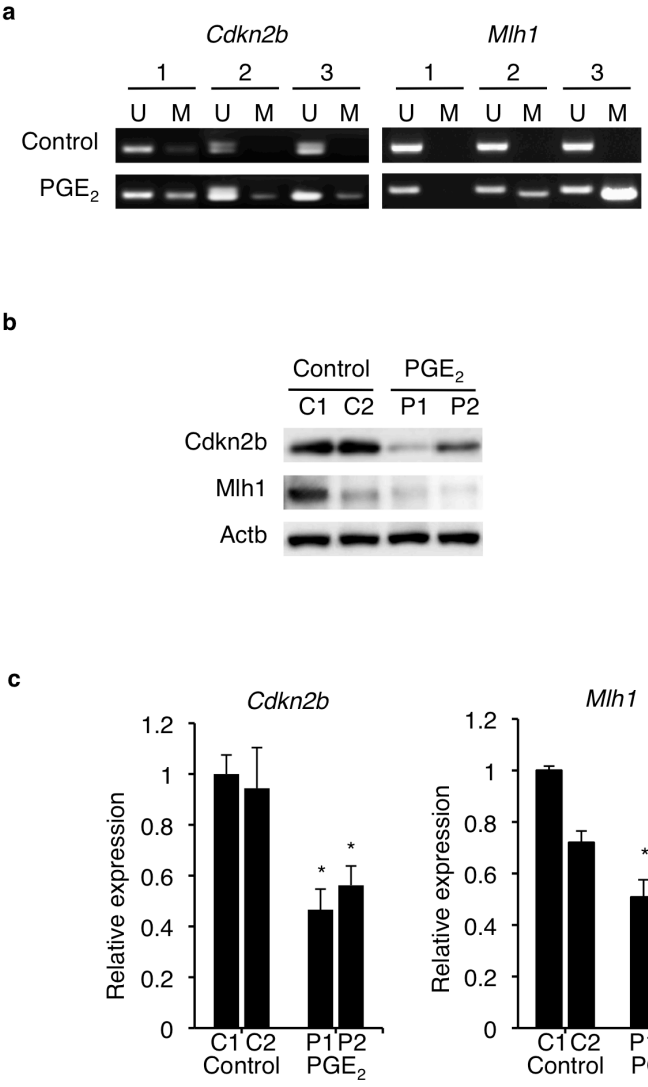

Supplementary Figure 3 PGE_2 promotes intestinal tumor growth via upregulating CGI methylation in *Apc*$^{Min/+}$ mice. (**a**) PGE_2 treatment increased the promoter CGI methylation of *Cdkn2b* (*p15*) and *Mlh1* in the colonic tumor epithelial cells isolated from a cohort of three male *Apc*$^{Min/+}$ mice for each group. The CGI methylation of *Cdkn2b* (*p15*) and *Mlh1* was examined by MSP as described in **Supplementary Fig. 2c**. (**b,c**) Treatment of *Apc*$^{Min/+}$ mice with PGE_2 decreased Cdkn2b (p15) and Mlh1 expression in colonic tumor epithelial cells. The Cdkn2b (p15) and Mlh1 expression at protein levels (**b**) and mRNA levels (**c**) from a cohort of two male mice for each group (C1 and C2 represent mouse treated with vehicle, P1 and P2 represent mouse treated with PGE_2) were examined. Error bars indicate s.d. * $P < 0.05$ (two-tailed unpaired Student's *t* test).

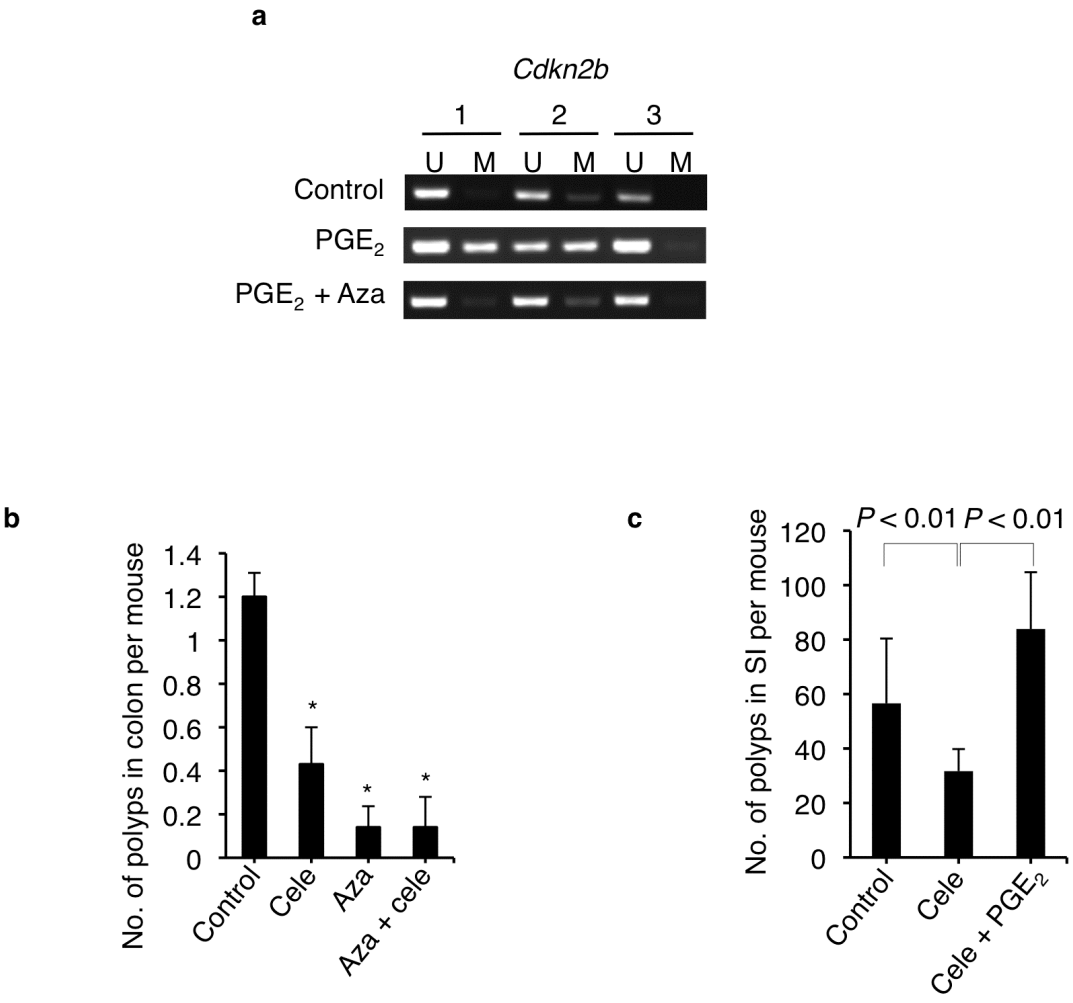

Supplementary Figure 4 The effects of a demethylating agent and celecoxib on PGE_2-enhanced CGI methylation and intestinal tumor growth. (**a**) Treatment of *Apc*$^{Min/+}$ mice with 5-Aza-dC attenuated PGE_2-enhanced CGI methylation of *Cdkn2b* (*p15*). The levels of CGI methylation of *Cdkn2b* (*p15*) in the colonic tumor epithelial cells isolated from a cohort of three male mice for each group were examined by MSP as mentioned in **Supplementary Fig. 2c**. (**b**) Combination treatment with celecoxib and 5-Aza-dC more efficiently inhibited colon tumor growth in *Apc*$^{Min/+}$ mice as described in **Fig. 2g**. Error bars indicate ± s.e.m. (*n* = 12, 14, 14, and 7, respectively). * *P* < *0.05* (Wilcoxon Rank Sum test). (**c**) PGE_2 reversed the effect of celecoxib on inhibiting tumor growth. Error bars indicate s.e.m. (*n* = 15 for each group. Wilcoxon Rank Sum test).

a

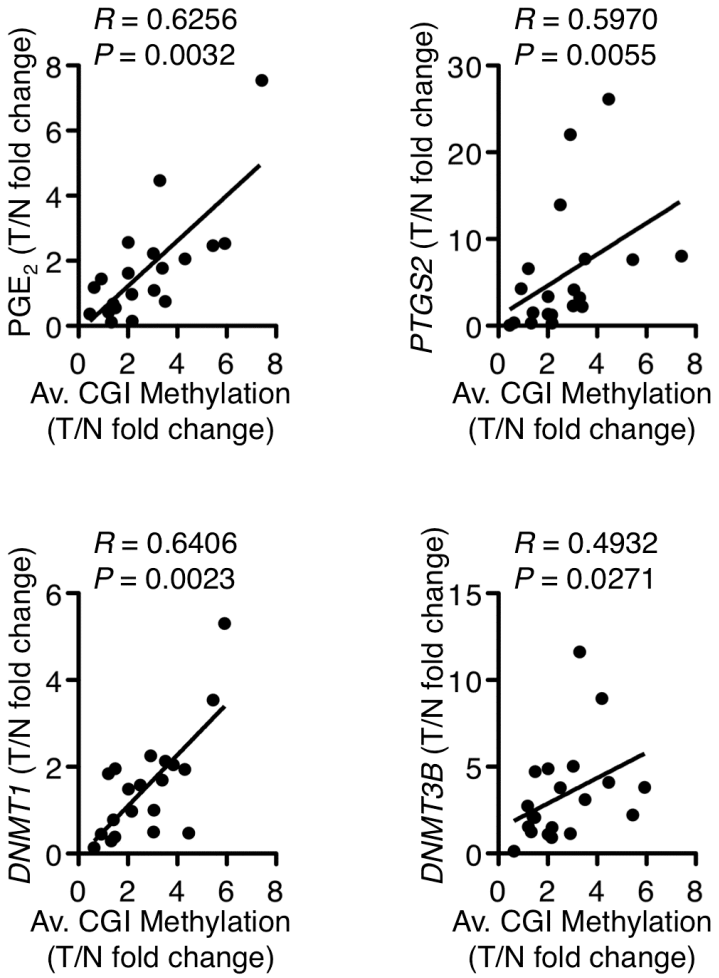
R = 0.6256
P = 0.0032
PGE2 (T/N fold change)
Av. CGI Methylation
(T/N fold change)
R = 0.5970
P = 0.0055
PTGS2 (T/N fold change)
Av. CGI Methylation
(T/N fold change)
R = 0.6406
P = 0.0023
DNMT1 (T/N fold change)
Av. CGI Methylation
(T/N fold change)
R = 0.4932
P = 0.0271
DNMT3B (T/N fold change)
Av. CGI Methylation
(T/N fold change)

b

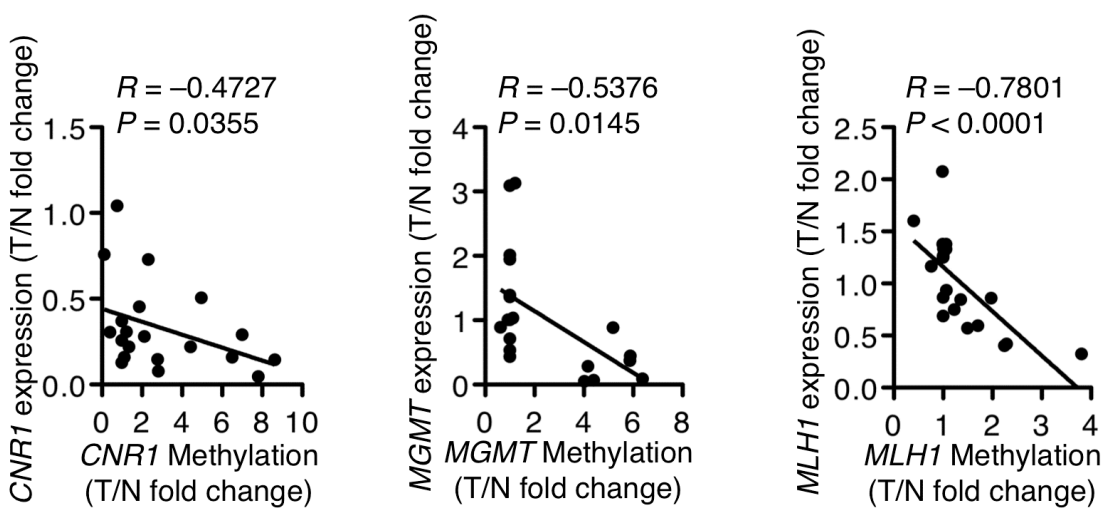
R = –0.4727
P = 0.0355
CNR1 expression (T/N fold change)
CNR1 Methylation
(T/N fold change)
R = –0.5376
P = 0.0145
MGMT expression (T/N fold change)
MGMT Methylation
(T/N fold change)
R = –0.7801
P < 0.0001
MLH1 expression (T/N fold change)
MLH1 Methylation
(T/N fold change)

Supplementary Figure 5 Correlation analysis between the levels of PGE_2, *PTGS2* (*COX-2*), *DNMT1*, *DNMT3B*, CGI methylation of target genes, and their expression. (**a**) The levels of PGE_2 and *PTGS2* (*COX-2*) expression were correlated with the CGI methylation in paired human tumor/normal tissues. The promoter CGI methylation of *CNR1*, *MGMT*, and *MLH1* were measured by bisulfite PCR sequencing. The average (Av.) of CGI methylation was the averaged CGI methylation of *CNR1*, *MGMT*, and *MLH1*. Data were presented as fold changes of tumor tissues as compared to matched normal tissues. Nonparametric Spearman correlation analysis (*R* value) was performed (n = 20). (**b**) Target gene expression reversely correlated with its CGI methylation. The expression of *CNR1*, *MGMT*, and *MLH1* was measured using Q-PCR. Data were presented as fold changes of tumor tissues as compared to matched normal tissues. Nonparametric Spearman correlation analysis (*R* value) was performed (n = 20) between the expression and CGI methylation of each target gene.

Supplementary Table

Table 1 Correlation of PGE_2, *PTGS2 (COX-2)*, *DNMT1*, *DNMT3B*, *CNR1*, *MGMT*, and *MLH1* with CGI methylation status in paired human tumor (T) and normal (N) tissues (Spearman *R* value and *P* value, *n* = 20). * indicates $P < 0.05$.

Methylation (T/N fold change)	Level/expression (T/N fold change)	*R*	*P*
CNR1	PGE_2	0.5668	0.0092*
	PTGS2 (*COX-2*)	0.6030	0.0049*
	DNMT1	0.5740	0.0042*
	DNMT3B	0.4619	0.0403*
MGMT	PGE_2	0.4096	0.0377*
	PTGS2 (*COX-2*)	0.4682	0.0159*
	DNMT1	0.4982	0.0155*
	DNMT3B	0.4998	0.0248*
MLH1	PGE_2	0.3734	0.1049
	PTGS2 (*COX-2*)	0.6230	0.0033*
	DNMT1	0.4402	0.0521
	DNMT3B	0.5182	0.0192*

Table 2 Primers used (U: unmethylated DNA; M: methylated DNA)

		Forward primers	Reverse primers	Ref.
Q-PCR primers				
ACTB		5'-AGAAAATCTGGCACCACACC-3'	5'-AGAGGCGTACAGGGATAGCA-3'	
CDKN2B		5'-AGGGATATTTAGGAGTGTGTGAC-3'	5'-CCATCGGAAGATTCGTAGCC-3'	
CNR1		5'-CGCAGGTCCTTACTCCTCAG-3'	5'-AGGACCCTGGTCCTGATCCT-3'	
DNMT1		5'-GAACCAACACCCAAACAG-3'	5'-TTCTCGTCTCCATCTTCG-3'	
DNMT3B		5'-TAACAACGGCAAAGACCGAGGG-3'	5'-TCCTGCCACAAGACAAACAGCC-3'	
MGMT		5'-CTTCACCATCCCGTTTTCC-3'	5'-TGCCTCTCATTGCTCCTC-3'	
MLH1		5'-CAGAATGTGGATGTTAATGTG-3'	5'-AGTCCTGGTAGCAAAGTC-3'	
PTGS2		5'-CCCTTGGGTGTCAAAGGTAA-3'	5'-GCCCTCGCTTATGATCTGTC-3'	
Cdkn2b		5'-GTGACATTGCGAGGTATC-3'	5'-GTAGGAAGTTATTTCTGATTGG-3'	
Cnr1		5'-CTGGTTCTGATCCTGGTGGT-3'	5'-TGTCTCAGGTCCTTGCTCCT-3'	
Gapdh		5'-GCCTTCCGTGTTCCTACC-3'	5'-GCCTGCTTCACCACCTTC-3'	
Mgmt		5'-TGCCTGCTCTCCATCACC-3'	5'-CTTCTCATTGCTCCTCCTACTG-3'	
Mlh1		5'-TGAGAGGTTCACTACGAG-3'	5'-TTCCATCTGAGTAACTTGC-3'	
Bisulfite PCR sequencing primers				
CDKN2B		5'-GGTTGGTTTTTTATTTTGTTAGAG-3'	5'-ACCTAAACTCAACTTCATTACCCTC-3'	
CNR1		5'-AGGGTAGGATAAAGGTTTATTAAT-3'	5'-CCCTTCCCAAACTCTTCACTAA-3'	
MGMT		5'-ATGTTGGGATAGTTCGCGTTTTTAGA-3'	5'-CCAATCCACAATCACTACAAC-3'	
MLH1		5'-GTGATAGATTAGGTATAGGGTT-3'	5'-AATATCCAACCAATAAAAACAAAAATA-3'	
Cnr1		5'-TTAGTGAGGTTTTGGTAATGAGTAG-3'	5'-TAAACCTTTATCCTACCCTAACAAC-3'	
Mgmt		5'-AGTGATTGGATTTTTAGTGGGTTTA-3'	5'-ATTCCTAAAACAAACCTCTTCTTCC-3'	
MSP primers				
CDKN2B	U	5'-TGTGATGTGTTTGTATTTTGTGGTT-3'	5'-CCATACAATAACCAAACAACCAA-3'	18
	M	5'-GCGTTCGTATTTTGCGGTT-3'	5'-CGTACAATAACCGAACGACCGA-3'	
MLH1	U	5'-TTTTGATGTAGATGTTTTATTAGGGTTGT-3'	5'-ACCACCTCATCATAA CTACCCACA-3'	18
	M	5'-ACGTAGACGTTTTATTAGGGTCGC-3'	5'-CCTCATCGTAACTACCCGCG-3'	
Cdkn2b	U	5'-GGTTTTTTATTTGGTGTGAGTTGT-3'	5'-CTCTAAAAACCCAATAACTTCAAT-3'	17
	M	5'-GTTTTTTATTCGGCGTGAGTC-3'	5'-CTCTAAAAACCCAATAACTTCGAT-3'	
Mlh1	U	5'-TTTGTTGTAGATGTTTGATTAGGGTTGT-3'	5'-CCACCTAATCACCTCTACTCAAAAACACA-3'	16
	M	5'-TCGTAGACGTTCGATTAGGGTCGC-3'	5'-TAATCGCCTCTACTCGAAAACGCG-3'	

DISCUSSION

Numerous genetic alterations have been reported in CRC, including *APC*, *KRAS*, *TP53*, *BRAF*, *PIK3CA*, and *PTEN*. Some of these mutations are associated with CIMP. For example, the levels of CIMP are associated with microsatellite instability (MSI) and mutations of *KRAS* and *BRAF* in CRC[1,2]. However, conflicting data exists over prognostic implications of CIMP in CRC[3,4]. This discrepancy may be due to the status of microsatellite stability (MSS) and *BRAF* mutations as well as biomarkers used for characterizing CIMP. For example, one report indicated that CRC patients with $CIMP^+$/MSS subtype had the worst clinical outcome and that this adverse prognostic effect depended on the presence of a BRAF mutation[5]. In contrast, another study reported that CIMP-high patients had shorter cancer-specific survival than CIMP-negative patients in the MSS subgroup and this correlation was lost after adjusting for the BRAF mutation[6], although the *BRAF* V600E mutation is associated with poor survival in CRC patients with MSS[7]. In addition, the KRAS mutation was reported to be more significantly associated with CIMP-low CRC than CIMP-high and CIMP-negative CRC after tumors were stratified by MSI status[8]. A subsequent study showed that this subtype of CRC (CIMP-low/KRAS-mutation) was correlated with worse prognosis[9]. Another recent study reported that CRC could be characterized into four distinct DNA methylation subgroups, including CIMP-high/BRAF-mutation, CIMP-low/KRAS-mutation, CIMP-negative/TP53-mutation, CIMP-negative/higher frequency of TP53 mutations, and CIMP-negative/low frequency of TP53 mutations[10]. Furthermore, RAS was found to affect epigenetic silencing through a pathway that is required for maintenance of a fully transformed phenotype[11]. Since *KRAS* and *BRAF* mutations contribute to CIMP in CRC, it is conceivable that the MAPK pathway could also influence CIMP in CRC. Indeed, a recent study showed that MAPK1 mutations were associated with a $CIMP^+$ and/or MSI^+ phenotype in CRC[12]. Our previous study showing that PGE_2 stimulated CRC cell proliferation via a RAS-MAPK pathway[13] prompts us to postulate that a RAS-BRAF-MAPK pathway may mediate the PGE_2 induction of DNMTs via its PTGER4 (EP4) receptor. Further

investigation is needed to test this hypothesis. Moreover, silencing of tumor suppressor and DNA repair genes by CGI methylation contributes to tumor initiation and progression although it may not directly be associated with poor survival in CRC patients.

METHODS

Materials and Reagents. LS-174T and HT-29 cells were purchased from ATCC. HCA7 cells were a generous gift from Susan Kirkland. These cells were maintained in McCoy's 5A medium containing 10% fetal bovine serum in a 5% CO_2 atmosphere and were cultured in serum free condition for 48 h before the treatments. For PGE_2 treatment, cells were treated with PGE_2 at 1 μM for 24 h. For celecoxib/PGE_2 treatment, cells were treated with PGE_2 at 1 μM after pre-treated with celecoxib at 10 μM for 72 h. For PTGER antagonist treatment, cells were pre-treated with 1 μM PTGER antagonist for 0.5 h before PGE_2 treatment (1 μM for 24 h). PGE_2 and CNR1 (CB1) antibody were purchased from Cayman Chemical. DNMT1, DNMT3B, and MLH1 antibodies were purchased from Santa Cruz Biotechnology. ACTB antibody and 5-Aza-dC were purchased from Sigma-Aldrich. MGMT and CDKN2B (p15) antibodies were purchased from Cell Signaling Biotechnology. Celecoxib was obtained from Pfizer.

Quantitative PCR. RNA was isolated from cultured cells or mouse colonic tumor epithelial cells using the TRIzol reagent and was reversely transcribed to cDNA using SuperScript III Reverse Transcriptase (Invitrogen). Q-PCR was performed with SYBR Green using the CFX96 Real-time System (Bio-Rad). *ACTB* and *Gpadh* were used as endogenous gene control. Primers used are listed in **Supplementary Table 2**.

Western blotting. Western blot analysis was performed as described previously[14].

Lentivirus production and stable transfection. DNMT1 and DNMT3B shRNAs were

purchased from Open Biosystems. Lentivirus production and stable transfection were performed as previously described[15].

Mouse experiments. *Apc*$^{Min/+}$ mice were purchased from Jackson Laboratory and were housed and treated in accordance with protocols approved by the Institutional Animal Care and Use Committee at The University of Texas M.D. Anderson Cancer Center. For PGE_2 treatment, male *Apc*$^{Min/+}$ mice at age of 4 weeks old were treated with PGE_2 at 100 μl of 1.5 μg μl^{-1} by gavage twice per day for 12 weeks. For combined treatment with PGE_2 and 5-Aza-dC, male *Apc*$^{Min/+}$ mice at age of 6 weeks old were treated with vehicle, PGE_2 as described above, or PGE_2 as described above plus 5-Aza-dC (1 mg kg^{-1}, IP injection, twice per week) for 8 weeks. For celecoxib and 5-Aza-dC treatment, male *Apc*$^{Min/+}$ mice at age of 6 weeks old were treated with vehicle, celecoxib (500 ppm in AIN-76A diet, MP Biomedicals), 5-Aza-dC as described above, or celecoxib plus 5-Aza-dC as described above for 13 weeks. For celecoxib and PGE_2 experiment, male *Apc*$^{Min/+}$ mice at age of six weeks old were treated with vehicle, celecoxib, or celecoxib plus PGE_2 as described above for 8 weeks. After the mice were sacrificed, the polyp number and size were counted and measured under a Nikon SMZ1000 dissecting scope using NIS-Elements imaging software.

Bisulfite PCR sequencing. Genomic DNA was isolated from cultured cells or mouse colonic tumor epithelial cells using QIAamp DNA Mini Kit (Qiagen). 500 μg of DNA was treated with sodium bisulfite using EZ DNA Methylation-Gold Kit (ZYMO Research). The bisulfite-converted DNA was amplified by PCR using Bio-Rad HotStar plus Taq DNA polymerase and primers listed in **Supplementary Table 2**. Cycling conditions were following: denaturation at 95 °C for 5 min, followed by 45 cycles of amplification (95 °C for 30 s, annealing temperature for 30 s, and 72 °C for 45 s), and a final extension at 72 °C for 10 min. The PCR products were run on a 3% agarose gel and recovered from the gel using QIAQuick Gel Extraction Kit (Qiagen). The

purified PCR products were submitted for sequencing (SeqWright) if their concentration was high enough or subjected to second round of PCR for further enrichment. On the chromatograms of sequencing results, the heights of methylated peak (C peak) and unmethylated peak (T peak) of each CpG were measured and the percentage of methylation was calculated as: methylation% =100 × value of methylated peak/(value of methylated peak + value of unmethylated peak). The overall DNA methylation of a gene promoter region was the average of methylation percentages of all CpGs examined.

Methylation-Specific PCR. Methylation-specific PCR (MSP) has been well established for measuring the status of specific CGI methylation of *CDKN2B* and *MLH1* genes in human CRC[16-18]. MSP analysis of bisulfite-converted DNA was performed using methylated (M) and unmethylated (U) primer sets listed in **Supplementary Table 2**. The cycling conditions were the same as for Bisulfite PCR Sequencing above. The PCR products were run on a 3% agarose gel and recovered with QIAQuick Gel Extraction Kit (Qiagen) after pictures were taken. The purified PCR products were submitted for sequencing (SeqWright) to confirm the methylation status of the amplified CpGs.

PGE_2 measurement. Tissues were homogenized in PBS with 10% 2,6-di-*tert*-butyl-*p*-cresol. PGE_2 level was measured using mass spectrometry and normalized with protein concentration.

Statistical analysis. The association studies with the human tumor and normal tissues were analyzed with nonparametric Spearman correlation analysis. The data generated from mouse experiments were analyzed with Wilcoxon Rank Sum test. The data generated from Q-PCR experiments were analyzed with two-tailed unpaired Student's *t* test. $P < 0.05$ was considered statistically significant.

REFERENCE

1. Shen, L.*, et al. Proc Natl Acad Sci U S A* **104**, 18654-18659 (2007).
2. Barault, L.*, et al. Cancer Res* **68**, 8541-8546 (2008).
3. Shen, L.*, et al. Clin Cancer Res* **13**, 6093-6098 (2007).
4. Ogino, S.*, et al. Gut* **58**, 90-96 (2009).
5. Kim, J.H., Shin, S.H., Kwon, H.J., Cho, N.Y. & Kang, G.H. *Virchows Arch* **455**, 485-494 (2009).
6. Dahlin, A.M.*, et al. Clin Cancer Res* **16**, 1845-1855 (2010).
7. Samowitz, W.S.*, et al. Cancer Res* **65**, 6063-6069 (2005).
8. Ogino, S., Kawasaki, T., Kirkner, G.J., Loda, M. & Fuchs, C.S. *J Mol Diagn* **8**, 582-588 (2006).
9. Yagi, K.*, et al. Clin Cancer Res* **16**, 21-33 (2010).
10. Hinoue, T.*, et al. Genome Res* (2010).
11. Gazin, C., Wajapeyee, N., Gobeil, S., Virbasius, C.M. & Green, M.R. *Nature* **449**, 1073-1077 (2007).
12. Slattery, M.L.*, et al. Carcinogenesis* **32**, 318-326 (2011).
13. Wang, D., Buchanan, F.G., Wang, H., Dey, S.K. & DuBois, R.N. *Cancer Res* **65**, 1822-1829 (2005).
14. Xia, D.*, et al. J Biol Chem* **282**, 3507-3519 (2007).
15. Xia, D., Holla, V.R., Wang, D., Menter, D.G. & DuBois, R.N. *Cancer Res* **70**, 824-831 (2010).
16. Borinstein, S.C.*, et al. Mol Carcinog* **49**, 94-103.
17. Wolff, L.*, et al. Oncogene* **22**, 9265-9274 (2003).
18. Xu, X.L.*, et al. World J Gastroenterol* **10**, 3441-3454 (2004).